DSMC Analysis of Cryogenic Hydrogen Expansion in Near-Vacuum Condition

Azam Che Idris[1], Mohd Rosdzimin Abdul Rahman[2]

[1] Faculty of Integrated Technologies, Universiti Brunei Darussalam

[2] Faculty of Engineering, Universiti Pertahanan Nasional Malaysia

Abstract

Hydrogen must be stored in a cryogenic temperature at high pressure to increase its energy density. Accidental release of cryogenic hydrogen must be studied before storage and handling safety code can be formulated. The present study simulated axisymmetric pin-hole release of hydrogen at 75 K, 50 K, 25 K and 15 K. The background pressure was set at 0.5 Torr with stagnation pressure at 750 Torr. The high-pressure ratio produced an under-expended shock structure which can be observed for all cases. The analysis was performed using the Direct Simulation Monte Carlo (DSMC) method which model the movement and collision of the gas particles. This code has been validated with experimental data of Nitrogen under-expansion at a similar pressure ratio. The results show that an inward dent formed on the Mach disc at very low temperature. This could be related to the recondensation effect of the flow due to rapid temperature decrease inside the barrel shock. At lower temperatures, the streamlines within the flow spread further apart in a radial direction which could enhance mixing with surroundings. The present work can contribute towards a well-informed hydrogen storage safety standard.

1. Introduction

Hydrogen fuel must be stored at a cryogenic temperature with high stagnation pressure to maximise its energy density. This requirement presented itself as an unknown hazard and potential high-risk situation. Unexpected or uncontrolled release of pressurized hydrogen is one of the physical aspects that go into consideration in developing hydrogen safety standards [1][2]. Its importance lies in determining the safe separation distances between a storage tank and its surroundings. There have been many studies on under-expanded hydrogen jet [3][4][5][6][7][8] but their analysis focused mostly on normal room temperature.

Experimental research on the sudden release of cryogenic hydrogen is limited due to the complex equipment setup needed. One experimental work described the axial concentration of hydrogen flowing through a 2 mm diameter nozzle from an 80 K reservoir [9]. In another work, Freidrich et al performed a similar measurement but at a lower temperature range of 34 – 65 K with stagnation pressure of 7 – 30 bar [10]. The numerical study by Giannissi [11] was validated by the Sandia National Laboratories data on cryogenic hydrogen release [5]. Most recently, Ba et al [12] performed numerical analysis using Navier-Stokes solver with Large Eddy Simulations (LES) turbulence model of cryogenic hydrogen jets released from round nozzles. They compared it with the experiment and found that the shock structures were satisfactorily simulated. In another study, Ichard et al [13] performed a CFD analysis of liquid hydrogen release and compared it experimental data. They focused mainly on the pooling of cryogenic hydrogen. However, it must be noted that all studies of cryogenic hydrogen release have primarily focused on relatively moderate pressure ratio only.

In our view, the high stagnation-to-background pressure ratio must be combined with the cryogenic temperature effect. The complex shape of a highly under-expanded jet can be affected by the cryogenic temperature effect. An example scenario, in a liquid-fuelled rocket, cryogenic hydrogen fuel is released from the fuel injector into a vacuum region before being ignited. This fuel injection has a stagnation-to-background pressure ratio of more than 1000 but their ignition depends of the

temperature of the gas. Any mishap in the ignition process could present a high risk for explosion or deviation in thrust vectoring. A similar situation can also happen in a cryogenic hydrogen tank. All cryogenic tank has an inner vacuum region that insulates the high-pressure inner vessel from the outer jacket. If the inner pressure vessel has a pinhole leak, the hydrogen will expand into the vacuum region before being in contact with the outer jacket. The leakage is highly under-expanded since the pressure ratio is very high. The temperature distribution of such jet must be known to choose a suitable distance and material for the outer jacket.

Recreating a situation of high-pressure expansion into the vacuum in an experiment is very hard due to the challenge of maintaining the vacuum pressure. Naturally, the vacuum region is being rapidly filled with incoming flow thus the overall pressure ratio change with time. This prompted researchers to rely on numerical analysis which can hold any boundary within the domain at the desired pressure. However, the presence of vacuum caused a breakdown in the continuity media assumption necessary to solve the Navier-Stokes equation. Thus, the published material in high-pressure gas expansion into vacuum relies on the concept of notional nozzle [3][9][11][14][15]. The general idea was to simulate only the downstream part where the jet has been stabilized and ignore the near-nozzle shock system.

Boyd et al [16] discussed the difficulty in modelling highly under-expanded flow in near-vacuum. The fluid is continuum upstream of the nozzle exit and becomes rarefied when it expands into the vacuum. Performing a traditional CFD analysis using Navier-Stokes solver can significantly underestimate important parameters such as heat transfer and drag force in the rarefied free jet. Boyd et al [16] found that DSMC fits the experimental data of nitrogen under-expansion into vacuum better than a Navier-Stokes solver. Other more recent works have also shown that the DSMC method can accurately model the jet expansion into vacuum [17][18][19][20]. Riabov and Fedoseyev [18] reported that DSMC is also capable of modelling the transitional and near-continuum regime upstream of the free jet expansion. This capability is expected since DSMC is considered more general than Navier-Stokes solver as the former models the movements of particles. The main challenge in using DSMC is the high computational cost and calculating particles movement in a continuum regime would render it impractical. That is the reason some researchers combine both Navier-Stokes solver and DSMC to model jet expansion into vacuum [21][22]. They modelled the continuum part in the nozzle using Navier-Stokes and combined it with DSMC at the rarefied jet downstream of the nozzle.

For our current analysis, we need to make sure that DSMC can model phase change since at 15 K the hydrogen is in the form of liquid before turning into gas during expansion. In the literature, DSMC has been reported to work well with phase change modelling [23][24][25][26]. This is expected since, in a practical sense, the difference between the vapour and liquid phase is mainly the distance between particles. In DSMC, the distance between particles is updated at every timestep since velocity and collision between particles are modelled. The same cannot be said with the continuum fluid model where the phase change is modelled by mass transport. For example, to simulate the boiling process, some mass of the liquid phase is transferred to the vapour phase.

In this current research, we have the objective of simulating a high-pressure ratio gas expansion at cryogenic stagnation temperature. This study can contributes towards formulating the safety of cryogenic hydrogen storage if the inner tank has small leakage in the vacuum flask.

2. Direct Simulation Monte Carlo

The code used in this current study followed the original Bird's DSMC code as presented in the [27]. He distributed the code as open-source through a personal website and users are allowed to modify the code to suit their own analysis.

The DSMC method simulates gas flow at the molecular level using the kinetic theory of gases. The state simulated molecules at any instance can be considered a function of the positions and velocities of every particle. The state of particles, presented as $X(t)$, is a function such of position and velocity for all particles which is presented as below:

$$X(t) = (r_1(t), V_1(t), \dots, r_N(t), V_N(t))$$

For each particle, the acceleration of each particle is a function of inter-molecules force plus external force. The inter molecules forces exist due to collisions depending on their initial trajectory and velocity.

In the original DSMC proposed by Bird, collisions between molecules are considered only if they belong to the same cell at the same time. To reduce the computational cost, collisions are random with an assigned probability value. However, the number of collision pairs we use in this analysis is different from Bird [27] and follow the paper by Boyd [28].

The procedure to calculate collision sampling is as follow. First, a pair of molecules is given the velocity vector of v_i and v_j before collision and v_i' and v_j' after collisions. To account for conservation of momentum:

$$mv_i + mv_j = mv_i' + mv_j'$$

For conservation of energy after a collision:

$$\frac{mv_i^2}{2} + \frac{mv_j^2}{2} = \frac{mv_i'^2}{2} + \frac{mv_j'^2}{2}$$

Velocities after a collision are to be assigned using the equation:

$$v_i' = v_i + [(v_j - v_i) \cdot \mathbb{m}]\mathbb{m}$$

$$v_j' = v_j - [(v_j - v_i) \cdot \mathbb{m}]\mathbb{m}$$

For hard-sphere molecules assumption, vector n is an isotropic random vector $[\mathbb{m}_x, \mathbb{m}_y, \mathbb{m}_z]$ where:

$$\mathbb{m}_x = \cos\theta = 1 - 2\alpha_1$$

$$\mathbb{m}_y = \sin\theta\cos(2\pi\alpha_2) = \sqrt{1 - \cos^2\theta}\cos(2\pi\alpha_2)$$

$$\mathbb{m}_z = \sin\theta\sin(2\pi\alpha_2) = \sqrt{1 - \cos^2\theta}\sin(2\pi\alpha_2)$$

α_1 and α_2 are random numbers generated with constant distribution between 0 and 1.

The interaction of particles with the wall boundary is described by the Maxwell model of specular scattering. Using this model, the molecule will maintain the original velocity except the direction will change after being reflected from the wall. Other than collision, moving particles can also interact with hard surfaces. All particles passing through permeable boundary are excluded from further calculation.

3. Numerical Case Setup

3.1 Code Validation Case

For validation of the numerical code, we will simulate the sudden expansion of nitrogen gas from 750 Torr reservoir going into 0.5 Torr near-vacuum chamber. The nitrogen is allowed to expand

through a 0.75 mm orifice. The temperature in the reservoir and ambient is set as 288 K. Similar analysis using CFD done by [29] will be used as a comparison. The expansion will be modelled inside a two-dimensional axisymmetric rectangular domain of the size 25 mm length and 11 mm height. The orifice is modelled as a very short nozzle with a length of 0.5 mm. All cells are uniformly rectangular with 0.4 mm for both height and length.

The mol_{wt} for Nitrogen is 28 and real particles per simulated particle is set as 1 X 10^{11}. The diameter is 4.1 X 10^{-10}.

3.2 Cryogenic Hydrogen Case

To simulate hydrogen cryogenic expansion into the near vacuum, we set utilise a similar mesh setup as before. However, the reservoir will be given temperatures of 75 K, 50 K, 25 K and 15 K whilst the temperature at ambient is kept at 288 K.

The mol_{wt} for Hydrogen is 2 and real particles per simulated particle is set as 1 X 10^{12}. The diameter is 2.88 X 10^{-10}.

4. Results

4.1 Validation Case

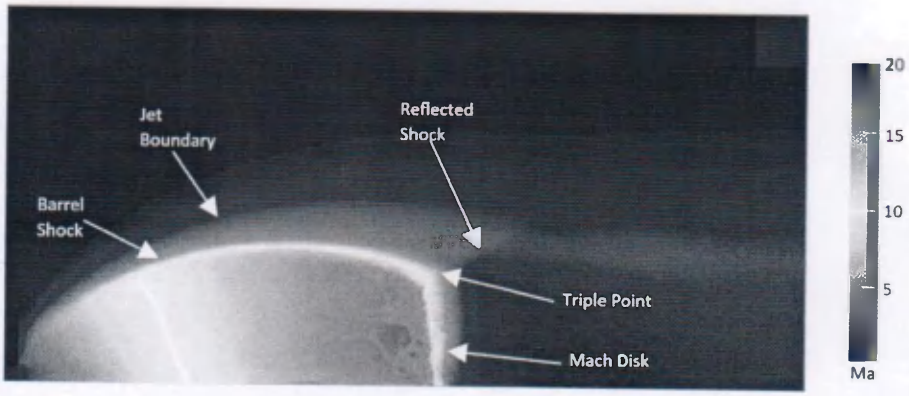

Figure 1: Under-expanded jet of Nitrogen gas (750 Torr, 288 K) release in near-vacuum (0.5 Torr)

Figure 1 above shows the under-expanded jet formation of the validation case. As high-pressure gas is expanded from the small orifice into low-pressure region, it will start to accelerate. This will create a distinctive bell-shaped jet with complex shock structures inside. Typically, the shock system includes a barrel shock, triple point, Mach disc, jet boundary and reflected shock. Inside the barrel shock, the flow accelerated via expansion waves formation until it reached the maximum Mach number. The Mach number of jet downstream of the reflected shock remains above supersonic whilst region downstream the Mach disk decelerated to subsonic. This large difference in speed of these two neighbouring regions caused a slip line to form in between.

The triple point location and Mach disc diameter measured using the image above are found to be about x_M = 18.8 mm and d_M = 11 mm. This is very close to the value found by Jugroot et al [29] which uses continuum CFD to model a similar setup. They reported that their CFD shows the two values around 19 mm and 11 mm. To further validate this simulation, we can compare it with the empirical value calculated using the formula given Ashkenas & Sherman [30] and French & Douglas [31]. Another by Zarvin et al [32] suggested the coefficient of 0.67 can be changed to 0.71

$$\frac{x_M}{d_o} = 0.67\sqrt{\frac{p_o}{p_b}}$$

$$\frac{d_M}{x_M} = 0.48$$

From the equation above, we can calculate that x_M = 19.6 mm and d_M = 9.4 mm. Thus we can conclude that our DSMC code can produce results closely similar to continuum CFD and experimental observation.

4.2 Mach Number of Cryogenic Hydrogen Under-expanded Release into Near-Vacuum

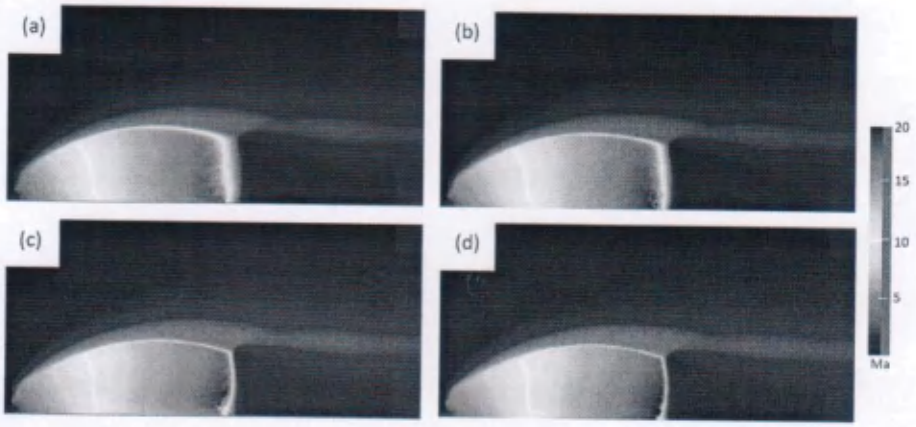

Figure 2: Mach number distribution of cryogenic hydrogen under-expansion release for (a) 75 K, (b) 50 K, (c) 25 K and (d) 15 K stagnation temperature

The shock structure for all cases can be seen clearly by the Mach number plot in the Figure 2 above. In general, the barrel shock shape is maintained by all cases even though their stagnation temperature varies significantly. Similarly, the maximum Mach number is kept at 20 without being influenced by temperature. The reason for this is due to the shock structure is mainly driven by the ratio of stagnation pressure and the background's static pressure.

At higher stagnation temperature, the normal shock looks smeared in comparison to the sharp and thin shock at low stagnation temperature. This due to the increase in the simulated number of particles for low-temperature cases. However, this does not produce significant errors in the location of the triple point.

At stagnation pressure of 25 K and 15 K, we can observe that the normal shock is curved near the mid symmetrical axis. We speculate that this is related to the condensation of the flow at that region such as has been observed in the experiment of cryogenic Nitrogen expansion into vacuum by Gartner et al [33].

4.3 Pressure of Cryogenic Hydrogen Under-expanded Release into Near-Vacuum

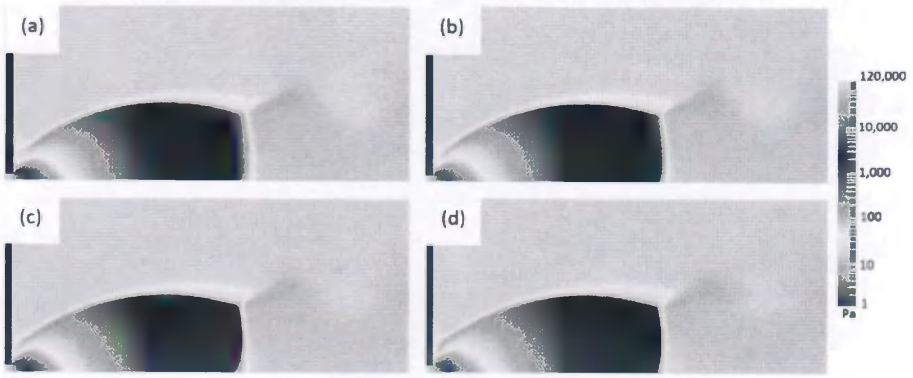

Figure 3: Static pressure distribution of cryogenic hydrogen under-expansion release for (a) 75 K, (b) 50 K, (c) 25 K and (d) 15 K stagnation temperature

The shape of the barrel shock and pressure distribution are the same for all cases. The pressure outside this shock formation is kept around 0.5 Torr. Inside the barrel shock, the pressure drops to almost zero just upstream of the terminating normal shock.

4.4 Temperature of Cryogenic Hydrogen Under-expanded Release into Near-Vacuum

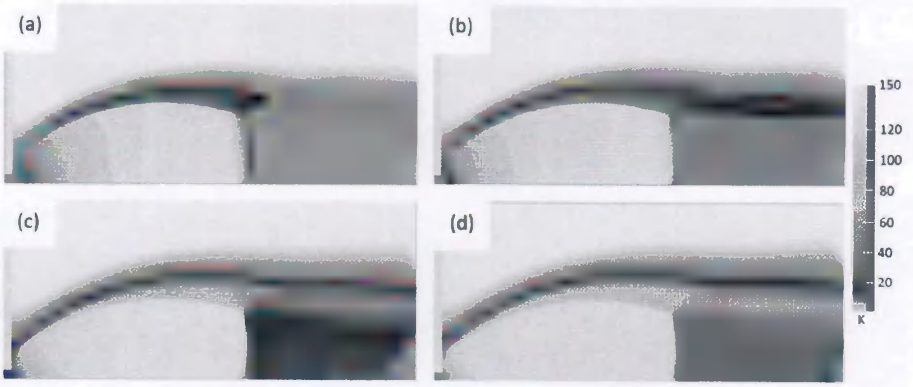

Figure 4: Static temperature distribution of cryogenic hydrogen under-expansion release for (a) 75 K, (b) 50 K, (c) 25 K and (d) 15 K stagnation temperature

Temperature plots of the whole flowfield for all cases are shown in figure 4. The colour scale has been set as such to show that temperature below 22 K will have a blue spectrum and beyond 22K will have an orange-yellow spectrum. Temperature 22 K is selected as the boundary in the colour scale as this temperature is the evaporation temperature of hydrogen at 1 bar. It can be observed that for all cases, the temperature reach below 22 K inside the barrel shock formation. The flow mostly maintains the gas phase in this region even though its temperature can reach as low as 5 K. Gas-phase is maintained due to the very low pressure inside.

In the case of 75 K stagnation temperature, the jet emanating downstream of the triple point have a core temperature of around 22 K. For all cases, the temperature downstream of the Mach disc equals the stagnation temperature. This means, there is a possibility of re-condensation to liquid downstream of the Mach disc. This can explain the inward dent on the Mach disc as observed for the case of 25 K and 15 K. There is even the possibility of solidification such as reported by Luo and Haidn [34]. They demonstrated that cryogenic liquid nitrogen and liquid methane can solidify when they are injected into vacuum.

4.5 Spray Expansion Cryogenic Hydrogen Under-expanded Release into Near-Vacuum

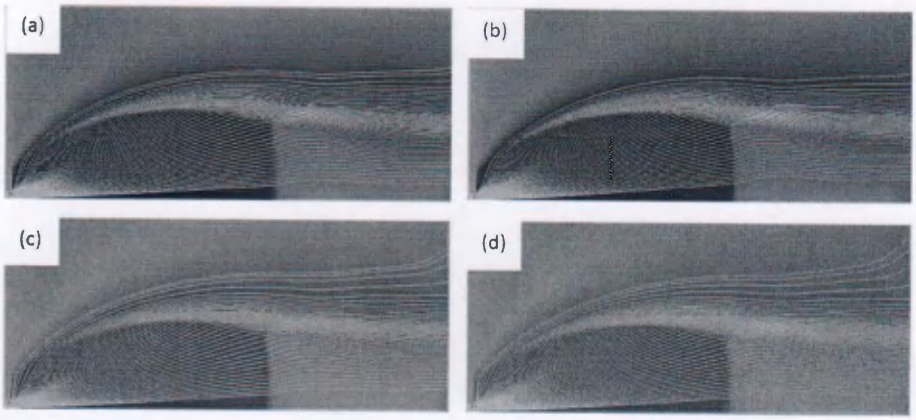

Figure 5: Static temperature distribution of cryogenic hydrogen under-expansion release for (a) 75 K, (b) 50 K, (c) 25 K and (d) 15 K stagnation temperature

The streamline for the flashing phenomena is shown in Figure 5 above. The seed number of streamlines is set sa 50 lines, originating from the nozzle exit. The streamlines are superimposed onto shadowgraph of the shock structures for easier identification any flow feature. At higher cryogenic temperature, the streamlines are more compact with each other. Bulk of the flow are confined within the jet surrounding the barrel shock. At lower cryogenic temperature, the streamlines are spread apart more. This is probably related to the larger temperature difference with the ambience.

5. Conclusion

DSMC code has been used to simulate sudden expansion of cryogenic hydrogen into near vacuum condition. The analysis has shown that the shape of the under-expanded jet is influenced more by the pressure ratio and less on the temperature. However, at very low temperature, the Mach disc could become dented at the mid-point, a phenomena similar to the re-condensation as observed by experiments on flashing cryogenic expansion. We also found that the temperature of the under-expanded jet is similar to the stagnation temperature in the hydrogen tank. This is true at least in the near nozzle region and a future study will be done in order to see the change in jet temperature further away from the nozzle.

References

1. Schefer RW, Houf WG, Williams T (2008) Investigation of small-scale unintended releases of hydrogen: momentum-dominated regime. International Journal of Hydrogen Energy 33:6373–6384.
2. Najjar YS (2013) Hydrogen safety: The road toward green technology. International Journal of Hydrogen Energy 38:10716–10728.
3. Li X, Christopher DM, Hecht ES, Ekoto IW (2017) Comparison of two-layer model for hydrogen and helium jets with notional nozzle model predictions and experimental data for pressures up to 35 MPa. International Journal of Hydrogen Energy 42:7457–7466.
4. Hu J, Christopher DM, Li X (2018) Simplified partitioning model to simulate high pressure under-expanded jet flows impinging vertical obstacles. International Journal of Hydrogen Energy 43:13649–13658.
5. Ruggles A, Ekoto I (2012) Ignitability and mixing of underexpanded hydrogen jets. International Journal of Hydrogen Energy 37:17549–17560.
6. Kotchourko N, Kuznetsov M, Kotchourko A, et al. (2014) Concentration measurements in a round hydrogen jet using Background Oriented Schlieren (BOS) technique. International journal of hydrogen energy 39:6201–6209.
7. Han SH, Chang D, Kim JS (2014) Experimental investigation of highly pressurized hydrogen release through a small hole. International journal of hydrogen energy 39:9552–9561.
8. Li X, Chen Q, Chen M, et al. (2019) Modeling of underexpanded hydrogen jets through square and rectangular slot nozzles. International Journal of Hydrogen Energy 44:6353–6365.
9. Xiao J, Travis J, Breitung W (2011) Hydrogen release from a high pressure gaseous hydrogen reservoir in case of a small leak. International journal of hydrogen energy 36:2545–2554.
10. Friedrich A, Breitung W, Stern G, et al. (2012) Ignition and heat radiation of cryogenic hydrogen jets. International Journal of Hydrogen Energy 37:17589–17598.
11. Giannissi SG, Venetsanos AG, Hecht ES (2021) Numerical predictions of cryogenic hydrogen vertical jets. International Journal of Hydrogen Energy 46:12566–12576.
12. Ba Q, He Q, Zhou B, et al. (2020) Modeling of cryogenic hydrogen releases. International Journal of Hydrogen Energy 45:31315–31326.
13. Ichard M, Hansen OR, Middha P, Willoughby D (2012) CFD computations of liquid hydrogen releases. International Journal of Hydrogen Energy 37:17380–17389.
14. Venetsanos A, Giannissi S (2017) Release and dispersion modeling of cryogenic under-expanded hydrogen jets. International Journal of Hydrogen Energy 42:7672–7682.
15. Velikorodny A, Kudriakov S (2012) Numerical study of the near-field of highly underexpanded turbulent gas jets. international journal of hydrogen energy 37:17390–17399.
16. Boyd Iain D, Penko PF, Meissner DL, DeWitt KJ (1992) Experimental and numerical investigations of low-density nozzle and plume flows of nitrogen. AIAA journal 30:2453–2461.
17. Wu J-S, Chou S-Y, Lee U-M, et al. (2005) Parallel DSMC simulation of a single under-expanded free orifice jet from transition to near-continuum regime.
18. Riabov V, Fedoseyev A (2013) The Analysis of Underexpanded Jet Flows for Hypersonic Aerodynamic Experiments in Vacuum Chambers. International Symposium on Shock Waves. pp 1561–1566
19. Ebrahimi A, Roohi E (2017) DSMC investigation of rarefied gas flow through diverging micro-and nanochannels. Microfluidics and Nanofluidics 21:18.
20. Chae J, Baek SW (2016) DSMC analysis of bipropellant thruster plume impingement on a geostationary spacecraft. Journal of Mechanical Science and Technology 30:4621–4632.
21. Rafi K, Fahd B, Deepu M, Rajesh G (2017) Experimental and Numerical Studies on the Plume Structure of Micro-nozzles Operating at High-Vacuum Conditions. International Symposium on Shock Waves. pp 927–936
22. Azizian P, Gorji-Bandpy M, Azarmanesh M (2018) Unsteady simulation of axisymmetric plume expansion into vacuum and its interactions with a rigid body with hybrid particle-continuum approach. Aeron Aero Open Access J 2:326–332.
23. Li Y, Xu S-L (2014) DSMC simulation of vapor flow in molecular distillation. Vacuum 110:40–46.
24. Venkattraman A, Alexeenko AA (2012) Direct simulation Monte Carlo modeling of metal vapor flows in application to thin film deposition. Vacuum 86:1748–1758.
25. Hu H, Huang J, Wu S, Yu P (2013) Simulation of vapor flows in short path distillation. Computers \& Chemical Engineering 49:127–135.
26. Bhandarkar M, Ferron JR (1991) Simulation of rarefied vapor flows. Industrial \& engineering chemistry research 30:998–1007.
27. Bird GA (1994) Molecular gas dynamics and the direct simulation of gas flows. Molecular gas dynamics and the direct simulation of gas flows
28. Boyd ID (1996) Conservative species weighting scheme for the direct simulation Monte Carlo method. Journal of Thermophysics and Heat Transfer 10:579–585.
29. Jugroot M, Groth CP, Thomson BA, et al. (2004) Numerical investigation of interface region flows in mass spectrometers: neutral gas transport. Journal of Physics D: Applied Physics 37:1289.
30. Ashkenas H, Sherman F (1966) Rarefied Gas Dynamics, ed. JH de Leeuw. New York: Academic p 84.
31. Douglas D, French J (1988) Gas dynamics of the inductively coupled plasma mass spectrometry interface. Journal of Analytical Atomic Spectrometry 3:743–747.
32. Zarvin A, Yaskin A, Kalyada V (2018) Effect of Condensation on the Length of Strongly Underexpanded Jets Exhausting Into a Rarefied Submerged Space. Journal of Applied Mechanics and Technical Physics 59:86–92.

33. Gärtner JW, Kronenburg A, Rees A, et al. (2020) Numerical and experimental analysis of flashing cryogenic nitrogen. International Journal of Multiphase Flow 130:103360.
34. Luo M, Haidn OJ (2016) Injection of cryogenic propellants under low pressure conditions. 52nd AIAA/SAE/ASEE Joint Propulsion Conference. p 4790